

Detection of 100 aM Fluorophores Using a High-Sensitivity On-Chip CE System and Transient Isotachopheresis

Byoungsok Jung,[†] Yonggang Zhu,[‡] and Juan G. Santiago^{*,†}

Department of Mechanical Engineering, Stanford University, Stanford, California 94305, and CSIRO Manufacturing and Infrastructure Technology, Highett, VIC 3190, Australia

We present a highly sensitive capillary electrophoresis (CE) assay that combines transient, single-interface on-chip isotachopheresis (ITP) and a laser-induced confocal fluorescence detection setup. We performed experimental parametric studies to show the effects of microscope objective specifications and intensity of excitation laser on optimization of a high-sensitivity on-chip CE detection system. Using the optimized detection system, single-molecule detection of Alexa Fluor 488 was demonstrated, and signal data were validated with autocorrelation analysis. We also demonstrated a separation and detection of 100 aM fluorophores (Alexa Fluor 488 and bodipy) in a fast assay using a high-sensitivity on-chip CE detection system and an ITP/CE protocol with no manual buffer exchange steps. This is, to the knowledge of the authors, the highest electrophoretic separation sensitivity ever reported.

On-chip capillary electrophoresis (CE) is one of the most widely used microchip assays and has been the subject of extensive research over the past decade.^{1–3} Translating CE methods from traditional capillary systems to a microchip platform provides several advantages including rapid separation, reduced sample volumes, and integration with other microfluidic functions. However, the limit of detection (LOD) of on-chip CE systems can be limited by associated small sample volumes and the shallow depth of etched or embossed channels (typically 10–20 μm), which limits path length available to photodetectors.

The most direct way of lowering LOD is improving intrinsic detection sensitivity of a CE system (e.g., use of high-efficiency photodetector). Enabled by advances in photodetectors, optical detection and investigations of single molecules have been rapidly developed over the past decade.^{4,5} Detection of single fluorophores in fused-silica capillaries⁶ and microchannels⁷ has been demon-

strated using laser-induced confocal fluorescence microscopy. Fluorescence correlation spectroscopy on a single-molecule level allows characterization of microscale flows,⁸ single-molecule imaging of cell surface systems,⁹ and investigation of protein transport.¹⁰ Lundqvist et al.¹¹ showed separation of 3 pM fluorescein and 3 pM 5-carboxyfluorescein with 14-fL detection volume using constricted fused-silica capillaries, and Fister et al.⁷ demonstrated separation of 15 pM rhodamine 6G and 30 pM rhodamine B with 0.9-fL detection volume using a microchip. The latter is, to our knowledge, the highest sensitivity on-chip CE assay without sample stacking. Foote et al. showed detection of 100 fM FITC-labeled ovalbumin using a two-step sample preconcentration process combining field-amplified sample injection and a microfabricated porous silica membrane, which is permeable to buffer ions but excludes electromigration of larger molecules (e.g., proteins).¹²

Another approach of improving sensitivity is to integrate an online sample stacking method. Electromigration-based sample stacking, such as field-amplified sample stacking (FASS)^{13,14} and isotachopheresis (ITP),^{15,16} is relatively easy to integrate with on-chip CE and leverages spatial gradients of electrophoretic velocity of sample analytes as effected by gradients in ion density, mobility, or solvent viscosity. For FASS, the highest signal enhancement factor has been typically limited to 1000-fold using capillaries^{17,18} and 100-fold using microchips.^{19,20} The highest reported ITP signal

* To whom correspondence should be addressed. E-mail: juan.santiago@stanford.edu. Fax: (650) 723-7657.

[†] Stanford University.

[‡] CSIRO Manufacturing and Infrastructure Technology.

(1) Bruin, G. J. M. *Electrophoresis* **2000**, *21*, 3931–3951.

(2) Auroux, P. A.; Iossifidis, D.; Reyes, D. R.; Manz, A. *Anal. Chem.* **2002**, *74*, 2637–2652.

(3) Landers, J. P. *Anal. Chem.* **2003**, *75*, 2919–2927.

(4) Moerner, W. E.; Fromm, D. P. *Rev. Sci. Instrum.* **2003**, *74*, 3597–3619.

(5) Dittrich, P. S.; Manz, A. *Anal. Bioanal. Chem.* **2005**, *382*, 1771–1782.

(6) Nie, S. M.; Chiu, D. T.; Zare, R. N. *Anal. Chem.* **1995**, *67*, 2849–2857.

(7) Fister, J. C.; Jacobson, S. C.; Davis, L. M.; Ramsey, J. M. *Anal. Chem.* **1998**, *70*, 431–437.

(8) Dittrich, P. S.; Schwille, P. *Anal. Chem.* **2002**, *74*, 4472–4479.

(9) Harms, G. S.; Cognet, L.; Lommerse, P. H. M.; Blab, G. A.; Kahr, H.; Gamsjager, R.; Spaink, H. P.; Soldatov, N. M.; Romanin, C.; Schmidt, T. *Biophys. J.* **2001**, *81*, 2639–2646.

(10) Terada, S.; Kinjo, M.; Hirokawa, N. *Cell* **2000**, *103*, 141–155.

(11) Lundqvist, A.; Chiu, D. T.; Orwar, O. *Electrophoresis* **2003**, *24*, 1737–1744.

(12) Foote, R. S.; Khandurina, J.; Jacobson, S. C.; Ramsey, J. M. *Anal. Chem.* **2005**, *77*, 57–63.

(13) Jacobson, S. C.; Ramsey, J. M. *Electrophoresis* **1995**, *16*, 481–486.

(14) Lichtenberg, J.; Verpoorte, E.; de Rooij, N. F. *Electrophoresis* **2001**, *22*, 258–271.

(15) Walker, P. A.; Morris, M. D.; Burns, M. A.; Johnson, B. N. *Anal. Chem.* **1998**, *70*, 3766–3769.

(16) Kaniansky, D.; Masar, M.; Bielicikova, J.; Ivanyi, F.; Eisenbeiss, F.; Stanislawski, B.; Grass, B.; Neyer, A.; Johnck, M. *Anal. Chem.* **2000**, *72*, 3596–3604.

(17) Zhang, C. X.; Thormann, W. *Anal. Chem.* **1996**, *18*, 2523–2532.

(18) Quirino, J. P.; Terabe, S. *J. Chromatogr., A* **1999**, *850*, 339–344.

(19) Yang, H.; Chien, R. L. *J. Chromatogr., A* **2001**, *924*, 155–163.

(20) Beard, N. R.; Zhang, C. X.; deMello, A. J. *Electrophoresis* **2003**, *24*, 732–739.

enhancement factor has been roughly 500-fold for microchip experiments^{21,22} and 5500-fold for capillaries.²³ These are prior to our recent work where we demonstrated a million-fold signal enhancement and detection and separation of 100 pM analytes using on-chip transient ITP method and its integration with CE.²⁴

In this note, we describe the development and performance of a high-sensitivity on-chip CE detection system and evaluate its performance in conjunction with on-chip transient ITP. The detection system uses laser-induced confocal fluorescence microscopy, and fluorescent signals were measured using an ICCD camera and a PMT. This note also presents a calibration of this system including its signal intensity dependence on microscope objective specifications and excitation laser power, which are crucial to the optimization of sensitivity. We demonstrate a separation and detection of 100 nM fluorophores (Alexa Fluor 488 and bodipy) in a fast assay using a high-sensitivity on-chip CE detection system and a single-interface ITP/CE protocol with no manual buffer exchange steps.²⁴

EXPERIMENTAL SECTION

Chemicals and Microchips. Alexa Fluor 488 (carboxylic acid, succinimidyl ester) and bodipy FL (STP ester, sodium salt) were purchased from Molecular Probes (Eugene, OR). Fluorescein (sodium salt) was purchased from J.T. Baker (Phillipsburg, NJ). *N*-Hydroxyethylacrylamide (HEA) was purchased from Cambrex Bio Science (Walkersville, MD). V-50 initiator (2,2'-azobis(2-amidinopropane) dihydrochloride) was purchased from Wako Chemical USA (Richmond, VA). We synthesized poly(*N*-hydroxyethylacrylamide) (PHEA) using free-radical polymerization in aqueous solution.²⁵ For ITP, trailing electrolyte (TE) and leading electrolyte (LE) consist of 5 mM HEPES (pH 7.0; Sigma, St. Louis, MO) titrated with sodium hydroxide and 600 mM NaCl (Fisher Scientific, Pittsburgh, PA) dissolved in deionized water, respectively. All electrolyte solutions were filtered prior to use with 200-nm pore syringe filters (Nalgene Labware, Rochester, NY).

We used a standard, cross-pattern glass microchip (channel dimensions are 50 μm wide and 20 μm deep) purchased from Micralyne (Alberta, Canada) and a cross-pattern injection-molded poly(methyl methacrylate) (PMMA) microchip sealed with a 100- μm -thick PMMA cover film (channel dimensions are 80 μm wide and 30 μm deep), which was provided to us by Aclara Bioscience (Mountain View, CA).

Instrumentation. Our high-sensitivity CE system mainly consists of an Ar ion laser (model 95; Lexel, Fremont, CA), an inverted epifluorescent microscope (IX70; Olympus, Hauppauge, NY), a PMT (H7422-40; Hamamatsu Photonics K.K., Shizuoka, Japan), and an intensified CCD camera (IPentaMAX; Roper Scientific, Trenton, NJ) with a 12-bit intensity digitization resolution (Figure 1). We used high numerical aperture objectives (60 \times , NA of 0.9 or 1.4; Olympus) and a filter set (Z488/10 \times , Z488RDC, and HQ535/50; Omega Optical, Brattleboro, VT) with peak excitation

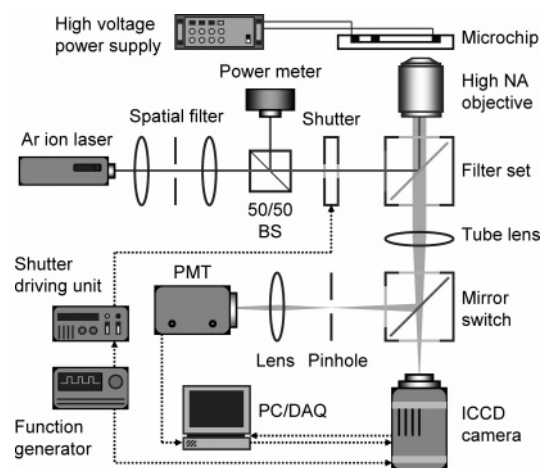


Figure 1. Schematic of the high-sensitivity on-chip CE system showing argon ion laser illumination, light filter, shutter, color filters, detectors, and data acquisition PC. Actuation of a mirror switch provides switching from an ICCD camera to a custom-built confocal system with a PMT.

and emission wavelength ranges of 483–493 and 510–560 nm, respectively.

Laser beam from the argon ion laser (488 nm) is focused into an iris diaphragm (1-mm diameter) and recollimated using a set of convex lenses ($f = 120$ mm) to remove unwanted multiple-order energy peaks and pass only the central maximum of the diffraction pattern of the laser beam. A power meter (13PEM001; Melles Griot, Carlsbad, CA) continuously measures intensity of laser beam from a 50/50 beam splitter. A microscope tube lens focuses collected fluorescence emission from the sample. Either an ICCD camera (for 2D imaging) or a PMT (for single-point confocal microscopy) can be used as a detector in this setup by actuating a switchable mirror. A 100- μm -diameter detection pinhole was placed at the focal plane of the tube lens to suppress out-of-focus rays, and a 10 \times objective (NA = 0.3; Olympus) to collect light passes the pinhole into the PMT. A pulse generator (model 555; BNC, San Rafael, CA) synchronizes a mechanical shutter (LS3ZM2 and VMMT1; Uniblitz, Rochester, NY) and the ICCD camera to minimize photobleaching of fluorescent samples. A LabVIEW-controlled high-voltage power supply (Micralyne, Alberta, Canada) was used to control the electric field for the ITP/CE process.

Sample Preparation. We carefully prepared sample solutions by serial dilution of stock solution. Glass bottles (volume of ~ 15 mL) were first washed with 30% hydrogen peroxide and then rinsed with DI water to avoid contamination. The concentration of stock solution was typically 1 μM ,²⁶ and we serially diluted this by 1/10 ratios (e.g., mixing 1 mL of 1 μM Alexa Fluor and 9 mL of buffer solution to make 100 nM Alexa Fluor solution) until we reached the desired concentration level. The lowest sample concentration used in this paper was 100 nM. We dispensed 100 μL into the chip reservoirs for each of our separation assays. The intensities of prepared sample solutions were also measured in order to calibrate the dilution process. We measured fluorescent signals of Alexa Fluor 488 (three independent lines of dilution ranging from 1 pM to 1 μM) in a glass microchannel. The normalized signal intensity of diluted sample solutions was linearly proportional to the sample concentration. This calibration validates

(21) Wainright, A.; Williams, S. J.; Ciambone, G.; Xue, Q. F.; Wei, J.; Harris, D. *J. Chromatogr., A* **2002**, *979*, 69–80.

(22) Jeong, Y. W.; Choi, K. W.; Kang, M. K.; Chun, K. J.; Chung, D. S. *Sens. Actuators, B: Chem.* **2005**, *104*, 269–275.

(23) Enlund, A. M.; Schmidt, S.; Westerlund, D. *Electrophoresis* **1998**, *19*, 707–711.

(24) Jung, B.; Bharadwaj, R.; Santiago, J. G. *Anal. Chem.* **2006**, *78*, 2319–2327.

(25) Albarghouthi, M. N.; Stein, T. M.; Barron, A. E. *Electrophoresis* **2003**, *24*, 1166–1175.

the sample dilution process and validates that normalized signal intensity data can be interpreted as measurements of absolute sample concentration. Photophysical properties of fluorophores are also important in the calibration process and the optimization of the detection system. For our lowest analyte concentration measurements, we chose Alexa Fluor 488 as a main sample analyte, as it has a high quantum yield, is more photostable than, for example, fluorescein and its conjugates, and is insensitive to pH changes within pH 4–9.²⁷

RESULTS AND DISCUSSION

In evaluating our high-sensitivity CE detection system, we focused on three parameters. First, we used either an ICCD camera or a high-efficiency PMT. Second, high NA objectives were used for high collection efficiency of emitted photons. Third, we optimized excitation laser power and the associated optical path so as not to overly saturate photon emission from fluorophores. We validated the signal intensity dependence on various parameters including sample concentration, C_s , exposure time of CCD camera, Δt , NA, and magnification (M) of objectives using an inverted epifluorescent microscope. The results confirmed that signal intensity (I) is proportional to the sample concentration, exposure time of CCD camera, and the fourth power of NA, and is also inversely proportional to the second power of the objective magnification: $I = AC_s \Delta t NA^4 M^{-2}$. For high sensitivity, high-NA objectives (e.g., oil immersion objectives) should be used with the lowest magnification compatible with the desired measurement. For example, the resolution, d_s (i.e., the point response function diameter) of an oil immersion objective with NA = 1.4) is 0.3 μm , which is smaller than the pixel dimension of our CCD using a 60 \times objective.²⁸ Therefore, magnifications greater than 60 \times can result in decreased sensitivity. Such considerations, of course, should be balanced with the working distance (WD = 0.25 mm) of the objective, which is often not compatible with many off-the-shelf microchips. In the data described below, we used a 60 \times water immersion objective (NA = 0.9, WD = 2 mm) for the glass microchips (cover glass thickness of 1 mm). Jung²⁹ presented a detailed discussion of our calibration procedures including a quantitative study of sensitivity for our detection system. Details are also given in the Supporting Information.

Figure 2 shows the measured relative signal-to-noise ratio (SNR) of two fluorescein concentrations together with predicted signal intensity as a function of excitation laser intensity. We define SNR as the ratio of peak intensity (above the background signal value) to twice the standard deviation of background noise. We also define relative SNR as SNR/ C_s and use it here to compare SNRs across different sample concentrations. Both the 1 and 10 pM cases clearly show that relative SNR increases as laser intensity increases in the low laser power, absorption-dominated

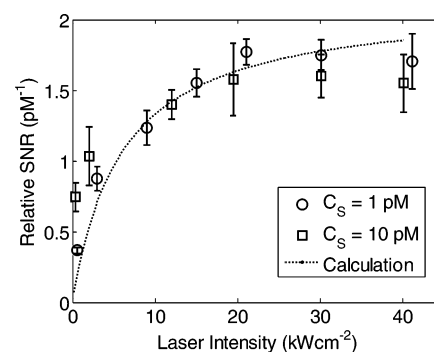


Figure 2. Relative SNR and calculated signal intensity of fluorescein as a function of excitation laser intensity. Relative SNR is defined as the ratio of SNR to the sample concentration. We used a 60 \times water immersion objective (NA = 0.9) and a simple cross-pattern glass microchip. The exposure time and frame rate of CCD camera was respectively 20 ms and 10 Hz. The error bars reflect 95% confidence intervals as determined from five realizations of each condition.

region. Relative SNR then saturates at higher laser power in a fluorophore-limiting region, where the fluorescence is saturated.³⁰ The $1/e^2$ waist of focused beam (r_0) was measured to be 4.0 μm , and laser power was varied from 0.1 to 20 mW. The effective probe volume (V_p) was estimated to be ~ 5.3 pL by taking into account electromigration of fluorescein molecules under an applied field ($E = 450$ V/cm): $V_p = h(\pi r_0^2 + 2r_0 \mu_{\text{FL}} E \Delta t)$, where h is the depth of microchannel, μ_{FL} ($= 3 \times 10^{-8}$ m²/V·s) is the electrophoretic mobility of fluorescein, and Δt ($= 20$ ms) is the exposure time of CCD camera. We suppressed electroosmotic flow to less than 4% of the bare-surface value using 0.1% w/v PHEA.^{24,25} For these data, we estimate that we collect signals from an average of approximately three molecules for the 1 pM sample concentration under the flowing conditions. The photon absorption and emission cycle rate (k_p) quantifies the fluorescent signal intensity and can be calculated using the equation, $k_p = 1/(\tau_f + 1/k_a)$, where τ_f is the excited-state life time and k_a is the absorption rate.³¹ We used photophysical parameters of fluorescein quoted from published data.³² ($\tau_f = 4.7$ ns, $k_a = 3.8 \times 10^{-3} \epsilon P / \pi r_0^2$, where ϵ is the molar extinction coefficient of fluorescein, P is the laser power, and r_0 is the radius of focused laser beam.) The predicted signal intensity shows fairly good agreement with the experimental data.

We demonstrated the performance of our high-sensitivity CE system using the highest NA objectives (60 \times oil immersion, NA = 1.4) and the PMMA microchip with a thin cover film. Figure 3 shows signal bursts from single and near-single molecules of Alexa Fluor 488 flowing in pressure-driven flow (bulk velocity of 1 cm/s). The left column in Figure 3 shows the background noises signal from deionized water, and the right column shows the signals from the 10 pM Alexa Fluor 488 sample. The measured $1/e^2$ waist of focused beam ($2r_0$) was 2.0 μm . For the 60 \times objective (NA = 1.4) and 100- μm pinhole used here, the $1/e^2$ probe depth ($2z_0$) is limited by spherical aberration of the objective in practice and is estimated to be ~ 3.0 μm based on the performance of similar confocal microscope setups.^{33,34} We performed an auto-

(26) We dissolved Bodipy FL sodium salt into DI water to make a stock solution, as it is soluble in water. Alexa Fluor 488 carboxylic acid was first dissolved in a small amount (100 μL for 5 mg of Alexa Fluor) of DMSO and then diluted with DI water to desired concentration of stock solution. Both dyes are fluorescent solutes and produced no known conjugates in our amine free buffer.

(27) Panchuk-Voloshina, N.; Haugland, R. P.; Bishop-Stewart, J.; Bhalgat, M. K.; Millard, P. J.; Mao, F.; Leung, W. Y.; Haugland, R. P. *J. Histochem. Cytochem.* **1999**, *47*, 1179–1188.

(28) Meinhart, C. D.; Wereley, S. T.; Santiago, J. G. *Exp. Fluids* **1999**, *27*, 414–419.

(29) Jung, B. Ph.D., Stanford University, Stanford, CA, 2006.

(30) Deschenes, L. A.; Bout, D. A. V. *Chem. Phys. Letters* **2002**, *365*, 387–395.

(31) Nie, S.; Chiu, D. T.; Zare, R. N. *Science* **1994**, *266*, 1018–1021.

(32) Song, L. L.; Hennink, E. J.; Young, I. T.; Tanke, H. J. *Biophys. J.* **1995**, *68*, 2588–2600.

(33) Schneider, M. B.; Webb, W. W. *Appl. Opt.* **1981**, *20*, 1382–1388.

(34) Palmer, A. G., III; Thompson, N. L. *Appl. Opt.* **1989**, *28*, 1214–1220.

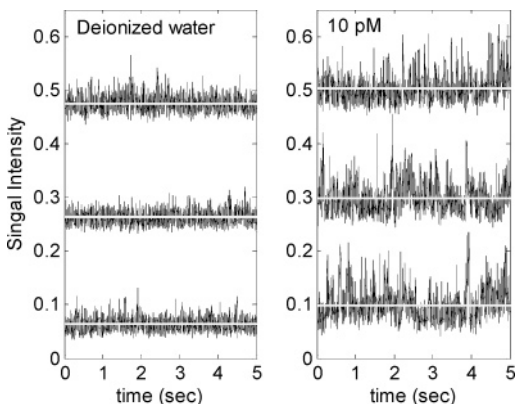


Figure 3. Instantaneous signals from single-molecule detection of Alexa Fluor 488. Left and right columns are respectively the signal intensity of DI water (with no buffer or sample ions) and 10 pM Alexa Fluor 488. Shown together with the data are horizontal gray lines showing the respective time-averaged value for each signal (the middle and top traces in each plot are offset by 0.2 and 0.4 AU, respectively). We used a PMMA microchip (microchannel cross-sectional dimensions are 50 μm wide and 20 μm deep) and 60 \times oil immersion objective (NA = 1.4). The excitation intensity of argon ion laser (488 nm) was 0.5 mW. Data acquisition rate was 50 kHz and temporal bin width 1 ms.

correlation analysis to verify that we achieved single-molecule sensitivity. The amplitude of the correlation function at zero time delay is proportional to the reciprocal of average number of molecules in the probe volume, and the decay of correlation represents the diffusion properties of molecules. The normalized correlation function, $G(\tau)$, can be expressed as

$$G(\tau) = \frac{\langle \delta I(t) \delta I(t + \tau) \rangle}{\langle I(t) \rangle^2} = \frac{1}{\langle N \rangle} \left(1 + \frac{4D\tau}{r_0^2} \right)^{-1} \left(1 + \frac{4D\tau}{z_0^2} \right)^{-0.5} \quad (1)$$

where δI is the fluctuation of fluorescence intensity, $\langle N \rangle$ is the average number of molecules in the probe volume, and D is the diffusion coefficient.³⁵ Although the temporal resolution of our data is not high enough to fully resolve diffusion properties, we can effectively bound the average number of molecules. We estimate an average of 0.6 fluorophores in the effective measurement volume for the data of Figure 3 (for an integration time of 20 μs).

Last, we demonstrated the effectiveness of our high-sensitivity CE system combined with our ITP/CE protocol to show separations of Alexa Fluor 488 and bodipy. The details of our ITP/CE protocol are presented in our previous work.²⁴ We used 600 mM NaCl and 5 mM HEPES as LE and TE, respectively. Figure 4 shows four separations of sample analytes (100 aM solutions each of Alexa Fluor 488 and bodipy) detected 30 mm downstream of the intersection with 40-s ITP stacking under a nominal electric field of 220 V/cm. Here, we used the cross-pattern borosilicate glass microchip. The electropherograms are determined by temporally binning (5-ms integration) PMT signals recorded at 1 kHz. The signal intensity was normalized with a background signal level, C_S , and a reference signal level as

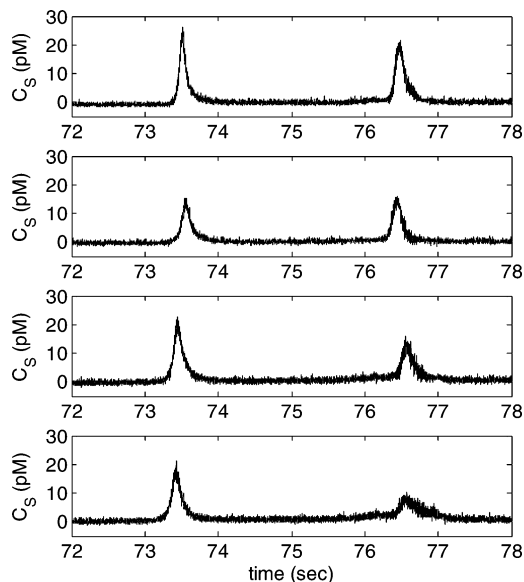


Figure 4. Four sample realizations of the electropherograms of ITP/CE separation of Alexa Fluor 488 (the peaks near 73.5 s) and bodipy (peaks near 76.5 s). We used a glass microchip (microchannel cross-sectional dimensions are 50 μm wide and 20 μm deep) and 60 \times water immersion objective (NA = 0.9). The detector was located at 30 mm downstream of the injection region of microchannel. The ensemble averaged SNR of the first and second peaks are approximately 50 and 39, respectively.

$$C_S = C_{\text{ref}}(I_{\text{raw}} - I_{\text{bg}})/(I_{\text{ref}} - I_{\text{bg}}) \quad (2)$$

where C_{ref} is the concentration of reference sample (10 pM) and I_{raw} , I_{ref} , and I_{bg} are respectively the signal intensities of stacked sample, reference sample, and background signal with no sample (the latter with shutter open and illumination as normal). We also prepared three independently diluted sample solutions using the serial dilution step described in the Experimental Section. For preparation of different sample solutions, we used the same initial stock solution of sample (1 μM) and the same DI water source in the same laboratory. The dilutions were otherwise independent including the day of preparation and the gloves, glassware, and pipet tips that were used. We carefully washed the microchannel before the loading of different sample solutions (5 min of DI water, 5 min of 0.1 M NaOH, 5 min of 1 M HCl, 5 min of 0.1% PHEA in DI water). We verified that the microchannels were not contaminated or that the experiments suffered from sample carryover (e.g., due to adsorption of sample onto channel walls) by running the ITP/CE protocol with a control buffer (sans sample). The results show that the stacking, separation, and detection process is repeatable for multiple experiments with independently prepared 100 aM sample solutions. For the data of Figure 4, the concentrations measured after injection, ITP stacking, and separation are respectively 21.4 and 15.9 pM for Alexa Fluor 488 and bodipy, as averaged across five realizations. This experiment achieves a concentration increase of 2.1×10^5 -fold relative to the initial sample concentration of 100 aM.

SUMMARY

We have developed a high-sensitivity on-chip CE detection system that leverages both optimized optics and a single-interface, transient ITP stacking protocol. In order to increase the intrinsic

(35) Rigler, R.; Elson, E. S. *Fluorescence Correlation Spectroscopy: Theory and Applications*; Springer: New York, 2001.

sensitivity of CE system, we chose high-efficiency photodetectors and performed extensive calibration studies of signal intensity dependence on excitation lasing power and objective specifications (NAs and magnifications). We used a high-NA objective with relatively low magnification (yet compatible with cover glass thickness of microchip) and optimization of laser power so as not to overly saturate sample analytes. We also used fluorophores with high quantum yield and photo and chemical stability. We demonstrated effective single-molecule detection of 10 pM Alexa Fluor 488 under pressure-flow conditions (bulk velocity of 1 cm/s) using an optimized laser-induced confocal fluorescence microscope setup fitted with 60 \times objective (NA of 1.4). We combined this high-sensitivity CE detection system and a single-interface,

transient ITP stacking method developed previously to show separation and detection of 100 aM concentrations each of Alexa Fluor 488 and bodipy. This is, to our knowledge, the highest sensitivity capillary electrophoresis separation and detection using either a microchip-based or traditional capillary CE system.

SUPPORTING INFORMATION AVAILABLE

Additional information as noted in text. This material is available free of charge via the Internet at <http://pubs.acs.org>.

Received for review May 23, 2006. Accepted September 29, 2006.

AC060949P